Effects of adiabatic electron trapping in collisionless electrostatic shocks

I. Pusztai[1], A. Sundström[1], J. M. TenBarge[2,3], J. Juno[4], and A. Hakim[3]

[1] *Department of Physics, Chalmers University of Technology, Göteborg, SE-41296, Sweden*

[2] *Department of Astrophysical Sciences, Princeton University, Princeton, NJ 08543, USA*

[3] *Princeton Plasma Physics Laboratory, Prinecton, NJ 08543, USA*

[4] *IREAP, University of Maryland, College Park, MD 20742, USA*

Electrostatic collisionless shocks appear in various laboratory and space plasmas; and they are also used in laser-plasma acceleration schemes to produce monoenergetic ion beams [1]. We investigate how the the existence and properties of low Mach-number electrostatic collisionless shocks are affected when the electron distribution function is flat in the trapped region, as is often the case due to an adiabatic trapping process. Besides corresponding modifications to the electron distribution our semi-analytical approach follows that of Ref. [2], which showed good correspondence to simulations with the Eulerian Vlasov-Maxwell solver of `Gkeyll` [3].

By assuming that the flattening of the electron distribution function is strictly linked to the minimum of the downstream potential oscillations we find solutions at higher Mach numbers than would be allowed by simple Maxwell-Boltzmann electrons, and more interestingly, we find regions of parameter space with multiple steady state electrostatic shock solutions.

Model We adopt a semi-analytical kinetic approach similar to Ref. [2], to describe the vicinity of the shock front in one-dimensional, steady state, electrostatic shocks. The sound speed $c_s = \sqrt{Z_i \hat{T}_e/\hat{m}_i}$ is defined with the charge number Z_j and mass $\hat{m}_i$ of the bulk ion species, and the electron temperature $\hat{T}_e$. Subscripts e, i, z, refer to electrons, bulk ions, and impurities, and j is a generic ion species index. A physical quantity $\hat{X}$ is normalized as $X = \hat{X}/\bar{X}$, where $\bar{X}$ is a species-independent normalizing quantity. In particular $\bar{T} = \hat{T}_i$ is the ion temperature, $\bar{n}$ is the bulk ion density of the unperturbed upstream plasma, $\bar{\phi} = \hat{T}_i/e$, $\bar{v} = \sqrt{\hat{T}_i/\hat{m}_p}$, with the proton mass $\hat{m}_p$, and $\bar{x} = \sqrt{\hat{T}_i \epsilon_0/(e^2\bar{n})}$, with the elementary charge e and the vacuum permittivity ϵ_0.

In the upstream region ($x > 0$) the potential ϕ drops from $\phi(x = 0) = \phi_{\max}$ to $\phi(x \to \infty) = 0$. In the downstream region ($x < 0$) it oscillates between $\phi_{\min}$ and $\phi_{\max}$. In the shock-frame, the far upstream ions have a velocity $-\hat{V}$, corresponding to a Mach number $\mathcal{M} = \hat{V}/c_s = \mathcal{O}(1)$, where $v_i = \sqrt{\hat{T}_i/\hat{m}_i}$ is the thermal speed of the main ions, and we assume $\hat{T}_e \gg \hat{T}_i \to \hat{V} \gg v_i$.

The distribution function f_j is constant along the contours of total energy $m_j v^2/2 + Z_j\phi$. The assumption of f_j to be a Maxwellian far upstream determines f_j in the passing and reflected regions of the phase space, while trapped and co-passing regions are assumed to be empty. Thus,

the ion densities are given by

$$n_j^{\pm}(x) = \int_{-\infty}^{\pm v_0} f_j dv \equiv \frac{n_j}{\sqrt{2\pi T_j/m_j}} \int_{-\infty}^{\pm v_0} dv \, \exp\left\{ -\frac{\left(\sqrt{v^2 + 2Z_j\phi(x)/m_j} - V\right)^2}{2T_j/m_j} \right\}, \quad (1)$$

where the $+$ and $-$ signs are relevant for the upstream and downstream, respectively; the speed at the phase space separatrices is $v_0(x) = \sqrt{[\phi_{\max} - \phi(x)]2Z_j/m_j}$, and n_j without argument is the density of the far upstream unperturbed plasma. ($n_i = 1 = T_i$ due to our normalization.)

Adiabatic trapping of electrons tend to produce a flat trapped electron distribution [4]. At which energy, $\phi_{\rm tr}$, this flattening happens depends on aspects of the shock that are outside the scope of our simple model: the far downstream potential variation and the time history of the shock. Here we assume the electron distribution to be constant for $\phi - m_e v^2/2 \geq \phi_{\rm tr}$, and Maxwell-Boltzmann for $\phi - m_e v^2/2 \leq \phi_{\rm tr}$, and take the plausible choice $\phi_{\rm tr} = \phi_{\min}$. This electron model (denoted by AD) corresponds to an electron density

$$n_e = n_{e1}\left[2\sqrt{\frac{\phi - \phi_{\rm tr}}{\pi T_e}}\exp\left(\frac{\phi_{\rm tr}}{T_e}\right) + \mathrm{Erfc}\left(\sqrt{\frac{\phi - \phi_{\rm tr}}{T_e}}\right)\exp\left(\frac{\phi}{T_e}\right)\right], \quad (2)$$

where $n_{e1} = \sum_j Z_j n_j^+(+\infty)$ represents the electron density far upstream, where $\phi = 0$ and the plasma is quasineutral, and according to (1), $n_j^+(+\infty) = \frac{n_j}{2}\left[1 + 2\mathrm{Erf}\left(\tilde{\mathrm{V}}_{\mathrm{j}}\right) + \mathrm{Erf}\left(\sqrt{\Psi_{\mathrm{j}}} - \tilde{\mathrm{V}}_{\mathrm{j}}\right)\right]$, where $\tilde{V}_j = V/\sqrt{2T_j/m_j}$, $\Psi_j = Z_j\phi_{\max}/T_j$.

Finally, the potential is calculated from Poisson's equation $\frac{d^2\phi(x)}{dx^2} = n_e(x) - \sum_j Z_j n_j(x) \equiv -\rho(x)$. The expressions for the densities depend parametrically on $\phi_{\min}$ and $\phi_{\max}$, which can be found employing Sagdeev potentials, $\Phi^+ = \int_0^{\phi} d\phi' \rho^+$, and $\Phi^- = \int_{\phi_{\max}}^{\phi} d\phi' \rho^-$. Solving the system $\{\Phi^+(\phi = \phi_{\max}, \phi_{\min}, \phi_{\max}) = 0, \Phi^-(\phi = \phi_{\min}, \phi_{\min}, \phi_{\max}) = 0\}$ gives $\phi_{\min}$ and $\phi_{\max}$.

Results In previous studies considering Maxwell-Boltzmann (MB) electrons it was found that above the threshold $T_e \approx 15$ there is a finite window of Mach numbers where solutions exist, and this window increases with T_e. For a given T_e, $\phi_{\max}$ and $\phi_{\min}$ monotonically increases with $\mathcal{M}$, as illustrated for $T_e = 200$ in Fig. 1a with red solid and dotted curves, respectively. However, when the trapped electron distribution function is assumed flat as explained previously, we find that above $T_e \approx 30$, the downstream potential extrema become multivalued functions of $\mathcal{M}$: there is a range of $\mathcal{M}$ with more than one solutions represented by the green/blue/black segments in Fig. 1a. Below this range only the smallest $\phi_{\max}$ solution (black) exists. Depending on the parameters, the highest $\phi_{\max}$ solution of the AD model (green)—that is usually very close to the MB result (red)—can extend above this region, or alternatively, as in this example, terminate somewhere inside the multivalued region.

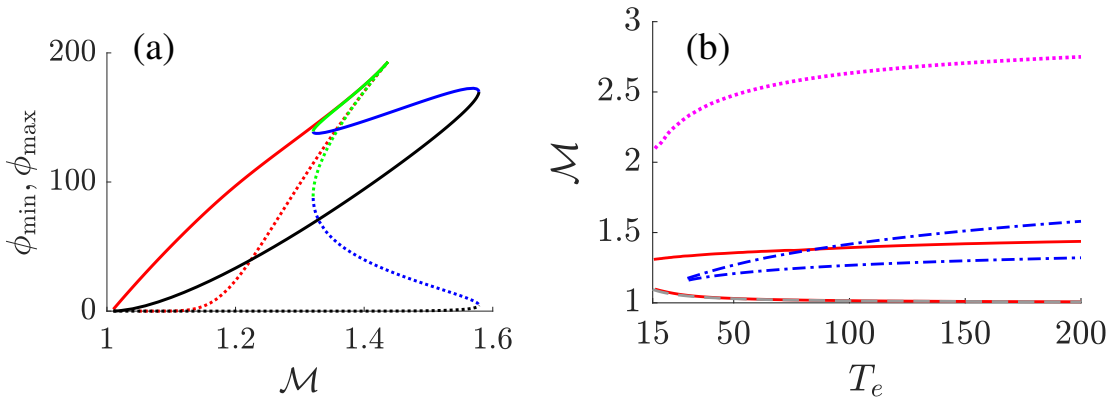

Figure 1: (a) $\phi_{\max}$ (solid) and $\phi_{\min}$ (dotted) as functions of $\mathcal{M}$ for $T_e = 200$. Red: MB electrons, green/blue/black: AD electron model roots with decreasing $\phi_{\max}$. (b) boundaries of the regions of existence for shock solutions. Solid: highest $\phi_{\max}$ root and MB model, dashed: theoretical lower limit, dash-dotted: multiple solutions exist, dotted: $\phi_{\rm tr} = 0$ (maximum effect of adiabatic electron trapping).

The boundaries of existence of various solution types are shown in Fig. 1b. The lower red curve is the limit of existence of shock solutions, that coincides with a more accurate expression for the sound speed accounting for finite ion pressure (dashed curve). The upper red curve corresponds to the upper limit of existence of the high $\phi_{\max}$ solution. At this threshold the amplitude of the downstream oscillation vanishes (and so do the trapped region of ions), thus the MB model predicts the same upper limit of existence. The boundary of the region where more than one solutions are allowed is shown with dash-dotted line. The upper boundary of the multivalued region surpasses that of the existence of the high $\phi_{\max}$ root at around $T_e = 85$, which means that steady state shock solutions exist at a higher Mach number than allowed by the MB model (which is the case in Fig. 1a).

The multivalued nature of $\phi_{\max}$ with Mach number is a consequence of that both decreasing $\phi_{\rm tr}$ (as for the upper dash-dotted curve in 1b) and decreasing the downstream oscillation of the potential (as for the upper solid curve) allows higher $\mathcal{M}$ solutions. As long as $\phi_{\rm tr}$ and $\phi_{\min}$ are strictly linked, these are competing requirements, but if the requirement $\phi_{\rm tr} = \phi_{\min}$ is relaxed, and large trapped regions and small oscillation are allowed in the same time, significantly higher values of $\mathcal{M}$ can be achieved: As an extreme reference case we show the boundary of existence for solutions at $\phi_{\rm tr} = 0$ with dotted line in Fig. 1b, appearing at significantly higher Mach number than allowed by the AD model.

The potential structures $\phi(x)$ of various solutions at $T_e = 200$ are shown in Fig. 2. Solutions of the AD model having the same $\phi_{\max} = 155$ are shown in Fig. 2a, with the same color coding for the various roots as in Fig. 1a. The "upper" root (green), which exhibits a small amplitude

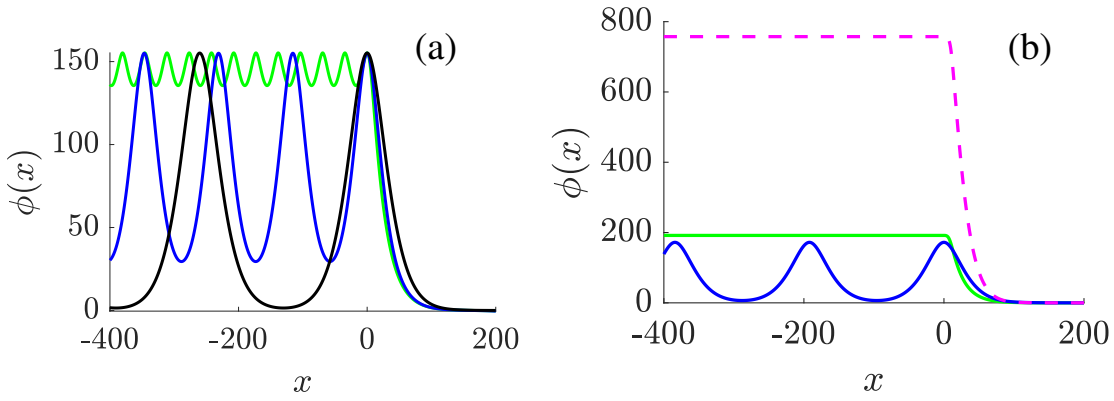

Figure 2: $\phi(x)$ for various shock solutions at $T_e = 200$. (a) Solutions of the AD model having the same $\phi_{\max} = 155$. (b) Highest Mach numbers solutions at this T_e. Green: upper root $\mathcal{M} = 1.44$, blue: middle root $\mathcal{M} = 1.58$, pink: $\phi_{\rm tr} = 0$, $\mathcal{M} = 2.75$.

oscillation, is very close to the MB electron solution (not shown), and it has $\mathcal{M} = 1.35$. The "middle" root (blue) has $\mathcal{M} = 1.45$ and its $\phi_{\min}$ is well separated from 0 and $\phi_{\max}$, while the "lower" root (black) has 1.56 and its $\phi_{\min}$ is almost 0: the solution is close to a solitary wave. It is interesting to observe this difference in the downstream behavior for the same shock size. This could mean that a shock initialization scheme might be very sensitive as to which type of shock is produced, which would be of high interest since the three different shocks in Fig. 1a have very different ion refection properties (a factor 10^6 between the green and the black solutions). The highest $\mathcal{M}$ solutions for $T_e = 200$ are shown in Fig. 2b. The downstream oscillation amplitude vanishes for the upper root (green), while it is significant for the degenerate middle/lower root (blue). The $\phi_{\rm tr} = 0$ case allows a significantly higher $\phi_{\max}$ and $\mathcal{M} = 2.75$ (pink).

Conclusions By assuming a flattening of the trapped electron distribution function with a trapping energy strictly linked to the minimum of the downstream oscillations in 1D laminar electrostatic shocks, we find that above an electron-to-ion temperature ratio of $T_e = 30$ multiple solutions are possible for the same temperature ratio and Mach number $\mathcal{M}$. The root that has the highest shock potential $\phi_{\max}$ is close to the result with Maxwell-Boltzmann (MB) electrons, while the two lower $\phi_{\max}$ roots exhibit strong downstream oscillations in ϕ. Above $T_e = 85$ the upper $\mathcal{M}$ limit of shock existence is extended above the MB result due to these roots.

References

[1] D. Haberberger et al., Nat. Phys. **8** 95 (2012).
[2] I. Pusztai et al., Plasma Phys. Control Fusion **60**, 035004 (2018).
[3] J. Juno et al., J. Comput. Phys. **353**, 110 (2018).
[4] A. V. Gurevich, Soviet Phys. JETP **26**, 575 (1968).